

# Surface Manipulation of the Electronic Energy of Subnanometer-Sized Gold Clusters: An Electrochemical and Spectroscopic Investigation

Yiyun Yang and Shaowei Chen\*

*Department of Chemistry, Southern Illinois University, Carbondale, Illinois 62901*

*Received September 24, 2002; Revised Manuscript Received November 7, 2002*

## ABSTRACT

Stable undecagold clusters were synthesized and protected with a monolayer of alkanethiolates. The particles were found to exhibit semiconductor electronic characteristics with a band gap of about 1.8 eV, as evaluated from voltammetric and spectroscopic measurements. Photoluminescence in the visible range was also observed from the peak position at 840 nm. The indirect band-gap characteristics indicate that there exist substantial surface trap states in the nanoparticle molecules. Prior to exchange reactions with alkanethiols, however, no luminescence was observed with the gold particles,  $\text{Au}_{11}\text{Cl}_3(\text{PPh}_3)_7$ . This was interpreted, at least in part, by the effect of ligand fields on the electronic (band-gap) energy splitting and the resulting electron distributions. These observations strongly suggest that surface chemistry plays a vital role in determining the electronic energy structure of these subnanometer-sized gold particles.

**Introduction.** The intense research interest in nanosized materials is mainly fueled by unique properties that are size-tunable, the so-called quantum effects. For instance, for both semiconductor and (transition-) metal nanoparticles, one interesting property is the growth (increase) of the band-gap energy with decreasing particle dimensions.<sup>1</sup> This provides powerful control of the materials' properties and consequently their potential applications, in particular, in the fields of optoelectronics, nanocircuits, nanodevices, et cetera.<sup>2</sup> Certainly these effects are much more apparent with semiconductor nanomaterials, as demonstrated previously, for instance, by the variation in the color of quantum dots with their sizes,<sup>3</sup> whereas for the metal counterparts, a sizable band gap can be observed only with much smaller nanoparticle dimensions.<sup>4,5</sup> For instance, earlier studies of alkanethiolate-protected gold nanoparticles<sup>5</sup> demonstrated that when the gold cores were smaller than 1.2 nm in diameter a HOMO–LUMO band gap started to evolve, as evidenced by voltammetric as well as near-IR measurements. In other words, in this size range, the gold nanoparticles started to exhibit semiconductor electronic characteristics. In these previous studies, the gold particles were synthesized by the Brust reaction,<sup>6</sup> with the core diameter readily varied within the range of 1 to 5 nm.<sup>7</sup> It can be anticipated that for smaller (i.e., subnanometer-sized) gold particles the semiconductor-like behaviors will be much more pronounced, for instance,

in terms of the electronic conductivity as well as the photoluminescence properties.<sup>8,9</sup>

Subnanometer-sized gold clusters have been synthesized previously and used mainly as biological labeling tags in electron microscopy measurements.<sup>10</sup> For instance, Bartlett et al.<sup>10</sup> reported the synthesis and biological application of undecagold clusters ( $\text{Au}_{11}$ , diameter 0.8 nm). In these earlier studies, the  $\text{Au}_{11}$  particles were protected by an amino-substituted triarylphosphine ligand, were generally not stable, and were prone to oxidative decomposition when exposed to ambient conditions. Recently, Hutchison and co-workers<sup>11</sup> employed an exchange-reaction route to replace the triphenylphosphine protecting shell with alkanethiols and obtained stable  $\text{Au}_{11}$  nanoparticles.

In this report, we used a slightly modified procedure to synthesize similar subnanometer-sized gold particles and carried out a series of spectroscopic and electrochemical studies. We observed that the electronic energy of these ultrasmall particles was very sensitive to the nature of the surface-protecting ligands and their bonding interactions with gold cores. For instance, the particle band gap was found to increase from 1.4 to 1.8 eV when surface-protecting ligands were varied from triphenylphosphines to alkanethiolates. Consistent results were also observed in photoluminescence and voltammetric measurements.

**Experimental Section. Chemicals.** Tetrachloroauric acid ( $\text{HAuCl}_4 \cdot x\text{H}_2\text{O}$ , Aldrich), tetrabutylammonium perchlorate (TBAP, 98%, ACROS), triphenylphosphine ( $\text{PPh}_3$ , 99%,

\* To whom all correspondence should be addressed. E-mail: schen@chem.siu.edu.

ACROS), and sodium borohydride ( $\text{NaBH}_4$ , 99+%, ACROS) were used as received. All solvents were obtained from typical commercial sources and were used without further treatment. Water was supplied by a Nanopure water system (18 M $\Omega$ ).

The synthetic protocol of  $\text{Au}_{11}$  nanoparticles was slightly different from that described by Bartlett et al.<sup>10</sup> In our approach, the precursor chloro(triphenylphosphine)gold(I) ( $\text{AuPPh}_3\text{Cl}$ ) was synthesized by following a literature procedure.<sup>12</sup> This was then used to produce gold nanoparticles,  $\text{Au}_{11}\text{Cl}_3(\text{PPh}_3)_7$ , upon reduction by  $\text{NaBH}_4$  in ethanol, similar to the method described by Bartlett et al.<sup>10</sup> The particle compositions were determined by elemental analysis (University of Illinois, Microanalytical Laboratory), and the experimental results (Au, 53.15%; P, 1.11%; Cl, 2.62%; C, 36.12%; H, 2.60%) were quite consistent with theoretical predictions (Au, 52.76%; P, 5.28%; Cl, 2.59%; C, 36.81%; H, 2.56%). The core size of the resulting particles, which was determined by transmission electron microscopy (TEM) measurements, was estimated to be around 0.8 nm, corresponding to a  $\text{Au}_{11}$  core structure.<sup>11</sup> Alkanethiolate protecting shells were then introduced by exchange reactions with varied feed ratios, as described by Hutchison et al.<sup>11</sup> Here, only those particles that remained soluble in the exchange media (e.g.,  $\text{CHCl}_3$ ) and that exhibited a core size similar to that prior to the exchange reactions, as determined by TEM measurements, were collected. The nanoparticles are very stable with the alkanethiolate protecting shells, as compared to those prior to the exchange reaction that are prone to oxidative decomposition when exposed to the atmosphere.

**Spectroscopy.** To detect the purity of the reaction intermediates and the particles at varied synthetic and processing stages,  $^1\text{H}$  NMR spectra were acquired with a Varian 300 NMR spectrometer by using a concentrated solution of the samples dissolved in  $\text{CDCl}_3$ . UV-vis spectroscopy studies were carried out with an ATI Unicam UV4 spectrometer. Photoluminescence properties were studied with a PTI fluorospectrometer. In these experiments, the particle solutions were prepared in  $\text{CHCl}_3$  at a concentration of less than 1 mg/mL.

**Electrochemistry.** Voltammetric measurements were carried out with a CHI 440 Electrochemical workstation. A Pt microelectrode ( $r = 25 \mu\text{m}$ ) was used as the working electrode, with a Ag/AgCl wire and a Pt coil as the quasi-reference and counterelectrode, respectively. Prior to use, the working electrode was polished with 0.05- $\mu\text{m}$   $\text{Al}_2\text{O}_3$  slurries and then cleansed by sonication in dilute  $\text{HNO}_3$ ,  $\text{H}_2\text{SO}_4$ , and Nanopure water successively. The electrolyte solution was deaerated with ultrahigh-purity nitrogen for at least 20 min and blanketed with a nitrogen atmosphere during the entire experimental procedure.

**Results and Discussion.** Previously, it has been shown that monolayer-protected nanoparticles exhibit molecular capacitor character, which is reflected in the quantized charging of the nanoparticle double-layer capacitance.<sup>5</sup> Figure 1 shows the cyclic (CV) and differential pulse voltammograms (DPV) of the  $\text{Au}_{11}$  nanoparticles obtained before

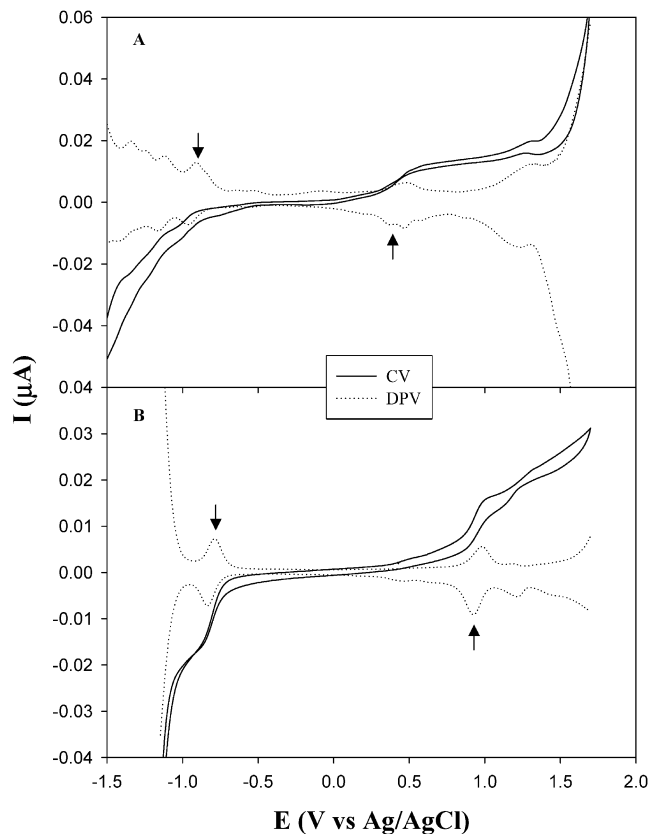


**Figure 1.** Cyclic (CVs) and differential pulse voltammograms (DPVs) of  $\text{Au}_{11}$  nanoparticles ( $\text{Au}_{11}\text{Cl}_3(\text{PPh}_3)_7$ ) before (A) and after (B) exchange reactions with *n*-dodecanethiols at a Pt microelectrode ( $25 \mu\text{m}$ ). The particle solutions were prepared in  $\text{CH}_2\text{Cl}_2$  with 0.1 M TBAP at concentrations of 0.5 mM (A) and 1.2 mM (B). The CV potential scan rate was 20 mV/s; in the DPV measurements, the DC potential ramp was 20 mV/s, and the pulse amplitude was 50 mV. Arrows indicate the first positive and negative voltammetric peaks.

(A) and after (B) exchange reactions with *n*-dodecanethiols at a Pt microelectrode ( $25 \mu\text{m}$ ). One can see that in both cases there are a series of very well-defined charging peaks within the potential range of  $-1.2$  to  $+1.8$  V. These are ascribed to the discrete charging of the nanoparticle molecules at the electrode interface. However, these peaks are not evenly spaced with a large featureless central gap. As demonstrated previously,<sup>5</sup> these observations can be accounted for by the molecule-like electronic-energy structure of the particles arising from their ultras small core dimensions, with a rather substantial HOMO-LUMO gap. This band gap corresponds to the potential spacing between the first negative and positive voltammetric peaks.<sup>5,13,14</sup> From Figure 1, one can see that prior to exchange reactions (A) these two peaks are located at  $-0.94$  and  $+0.47$  V whereas after the exchange reaction with *n*-dodecanethiols (B), at  $-0.81$  and  $+0.95$  V (indicated by arrows), corresponding to effective band gaps of about 1.41 and 1.76 eV, respectively. For comparison, the band gap of butanethiolate-protected  $\text{Au}_{38}$  particles<sup>5</sup> was found to be approximately 0.9 eV, and that of  $\text{Au}_{55}(\text{Ph}_2\text{PC}_6\text{H}_4\text{SO}_3\text{H})_{12}\text{Cl}_6$ , 0.8 eV.<sup>15c</sup> This indicates that whereas the gold core dimensions remain virtually unchanged before and after exchange reactions the particle

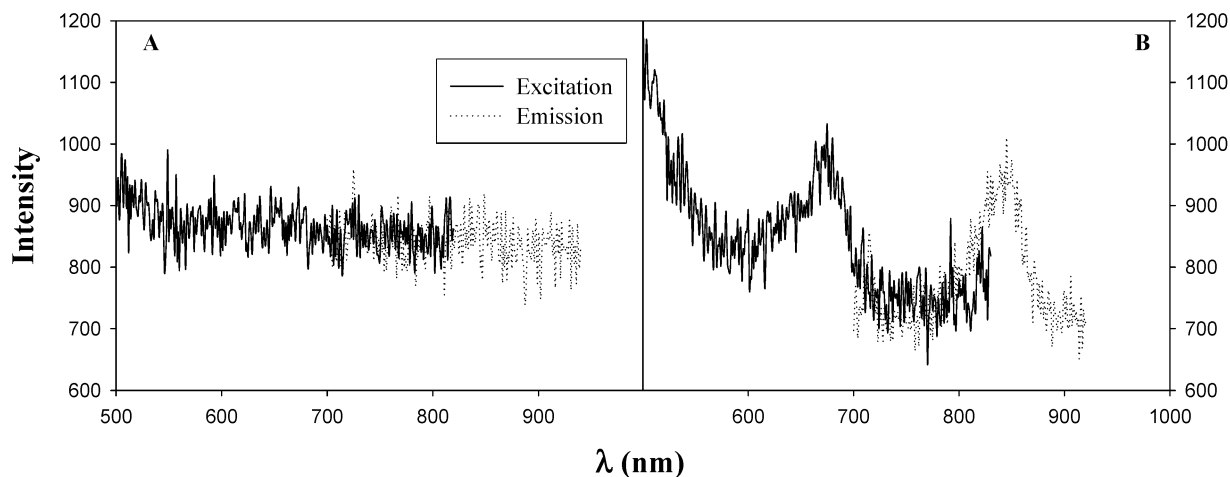


**Figure 2.** Excitation and emission spectra of undecagold clusters before (A,  $\text{Au}_{11}\text{Cl}_3(\text{PPh}_3)_7$ ) and after exchange reaction with dodecanethiols (B,  $\text{Au}_{11}\text{Cl}_2$ ). Excitation spectra were collected at  $\lambda_{\text{EM}} = 840$  nm, and emission curves were acquired when particles were excited at 680 nm. Particles were dissolved in  $\text{CH}_2\text{Cl}_2$  at concentrations of  $9.8 \mu\text{M}$  (A) and  $2.85 \mu\text{M}$  (B).

band gap increases by about 0.35 eV upon the replacement of the phosphine (and chloride) ligands by dodecanethiolates. This observation can be attributed to the stronger bonding of Au–S compared to that of Au–P (Cl),<sup>16</sup> which is akin to ligand-field effects on the splitting of the electronic energy of coordinated complexes.<sup>17</sup>

In addition, from these measurements, one can also estimate that the nanoparticle Fermi level shifts from  $-0.23$  V to  $-0.07$  V. One possible interpretation is that prior to exchange reactions the relatively weak ligand field in  $\text{Au}_{11}\text{Cl}_3(\text{PPh}_3)_7$  particles leads to more electrons residing in the conduction band (equivalent to a high-spin state); consequently, the Fermi level is somewhat more negative whereas after exchange reactions with *n*-dodecanethiols electrons are more likely to be degenerated, residing in the lower-energy valence band because of the strong ligand field (i.e., low-spin state). Thus, the Fermi level is located nearly halfway between the conduction band and the valence band. This interpretation is further supported by the charge-transfer characteristics between surface gold atoms and protecting ligands. It is known that P (in  $\text{PPh}_3$ ) can be an electron donor, leading to an increase in the electron density of the gold core and hence an upward (negative) shift of the Fermi level.<sup>15</sup> Opposite behaviors are anticipated from thiol protecting ligands, which behave as electron acceptors, resulting in a decrease in the gold core-electron density. These voltammetric measurements were carried out with the as-produced nanoparticles. The appearance of clear quantized charging features indicates that the nanoparticles are highly monodisperse, even without any postsynthesis fractionation.<sup>4</sup>

With such a large band gap, it is anticipated that these  $\text{Au}_{11}$  nanoparticles will also exhibit interesting photoluminescence properties.<sup>8,9</sup> Recently, the Whetten<sup>8</sup> and Murray<sup>9</sup> groups separately reported the observation of near-infrared to visible fluorescence from nanosized gold nanoparticles ( $<1.8$  nm in diameter). They interpreted the near-infrared luminescence by the HOMO–LUMO electronic transition of lower energy than that of the d–sp interband transition whereas the visible emission was ascribed to the interband

transitions between the filled  $5d^{10}$  band and the  $6sp^1$  conduction band. Figure 2 shows the excitation and emission spectra of the  $\text{Au}_{11}$  nanoparticles obtained above. For  $\text{Au}_{11}$  nanoparticles that were protected with a monolayer of *n*-dodecanethiolates (panel B), a rather well-defined excitation peak can be observed at 680 nm (spectrum collected at  $\lambda_{\text{em}} = 840$  nm) and an emission peak at 842 nm (1.5 eV) when excited at 680 nm (1.8 eV). There are at least three aspects that warrant attention here. First, the rather substantial difference (0.3 eV, 160 nm) between the excitation and emission peak energies indicates that the particles behave as indirect band-gap semiconductor materials with rather significant (surface) trap energy states. One might also note that the excitation peak energy is very close to the band gap estimated voltammetrically (Figure 1). Second, the luminescence (emission) peak position red shifts rather drastically as compared to that observed with much larger particles used in Murray's study (1.8 nm in diameter).<sup>9</sup> At first glance, this is rather counterintuitive, as one would anticipate a blue shift of the luminescence energy with decreasing particle core size.<sup>1</sup> This discrepancy might be explained, at least in part, by the extremely small core size of the  $\text{Au}_{11}$  particles where all but one gold atom in the core are residing on the core surface. Consequently, the particle energy is mostly determined by surface states. Third, it should be mentioned that prior to the exchange reactions with alkanethiols the  $\text{Au}_{11}$  nanoparticles (with a protecting shell of triphenylphosphine,  $\text{Au}_{11}\text{Cl}_3(\text{PPh}_3)_7$ ) do not exhibit any luminescence response in the visible range (panel A) despite the fact that the core size remains virtually unchanged in the exchange reactions. It should also be noted that for these particles, whereas the band gap is estimated to be around 1.41 eV from the above voltammetric measurements (Figure 1A), no excitation peak was observed at 881 nm, indicating that there was no excitonic transition. Again, this might be attributable to the high-spin electronic structure in a weak ligand field. These observations strongly suggest that surface-bonding chemistry plays a vital role in regulating the fluorescence (electronic energy) properties of ultrasmall nanosized particles. In a

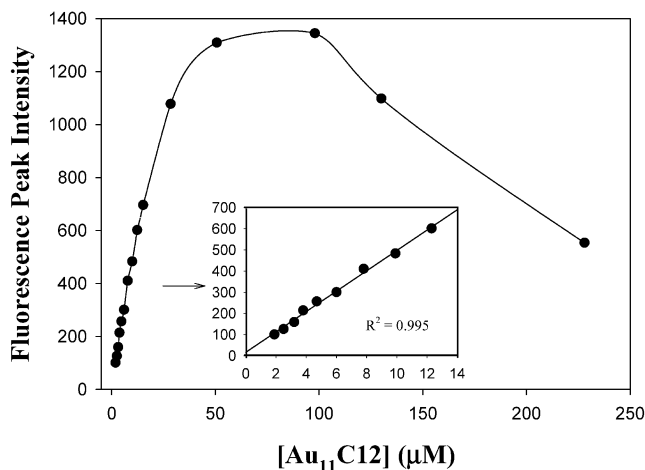


**Figure 3.** Variation of the fluorescence peak intensity of the Au<sub>11</sub>C12 particles (in Figure 2) with particle concentration. The line is only a guide for the eye. The inset shows the enlarged profile within the concentration range of 2 to 14 μM, where the symbols represent the experimental data and line is the linear regression.

previous study involving much larger gold nanoparticles,<sup>9</sup> the wavelength and efficiency of luminescence were found to vary with the specific protecting ligands (all involved in Au–S bonding linkages).

Figure 3 shows the variation of the fluorescence peak intensity of these Au<sub>11</sub>C12 particles with particle concentration. One can see that the luminescence intensity initially increases linearly with concentrations at [Au<sub>11</sub>C12] < 14 μM and reaches a maximum at about 100 μM. However, a further increase in the particle concentration leads to an apparent decrease in the particle fluorescence, probably due to self-absorption effects. Solvents do not seem to have a substantial impact on the fluorescence properties of these particles. For instance, the fluorescence profile and intensity were virtually unchanged when the particles were dissolved in CHCl<sub>3</sub> or methanol, presumably because of the alkanethiolate protecting monolayers that largely defined the nanoparticle surface dielectric properties (also, no drastic variation was observed when the particle protecting monolayers were changed from *n*-dodecanethiolates to *n*-hexanethiolates; not shown).<sup>18</sup> Overall, the fluorescence intensity is about 4 orders of magnitude smaller than that observed by Murray and co-workers with tiopronin-protected gold particles (1.8-nm diameter) at comparable particle molar concentrations.<sup>19</sup> This lower quantum efficiency of photoluminescence can be ascribed to surface trap states, as speculated above.

The nanoparticle electronic energy structure can also be investigated by using UV–visible spectroscopy. Figure 4 shows the corresponding UV–visible spectra acquired with the same solutions used in fluorescence measurements (Figure 2). The overall features are quite consistent with those shown in Hutchison’s work<sup>11</sup> except that in the present study a much wider wavelength range was probed. It can be seen that after exchange reactions with *n*-dodecanethiols the gold particles exhibited a rather large absorption band at 676 nm (1.83 eV) in addition to the two major peaks at 370 and 416 nm, which were observed with the preexchange particles (Au<sub>11</sub>Cl<sub>3</sub>(PPh<sub>3</sub>)<sub>7</sub>) as well. The latter two most probably arise

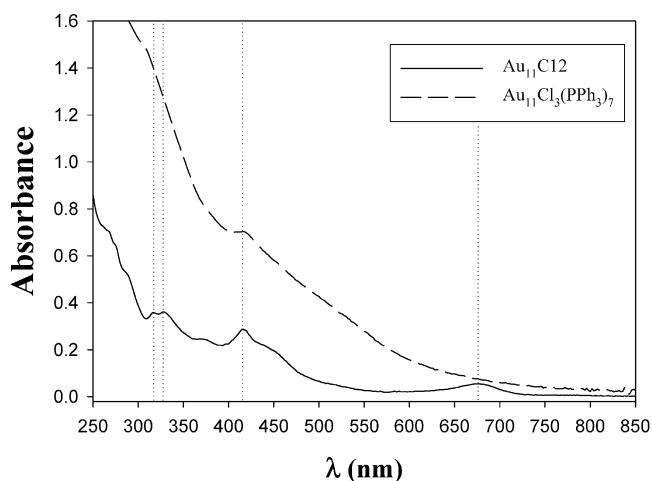


**Figure 4.** UV–visible spectra of undecagold clusters before (Au<sub>11</sub>Cl<sub>3</sub>(PPh<sub>3</sub>)<sub>7</sub>) and after exchange reactions with dodecanethiols (Au<sub>11</sub>C12). The particle concentrations were the same as those in Figure 2.

from the nanoparticle interband electronic transitions whereas the peak at 676 nm is equivalent to the excitonic transition observed with semiconductor quantum dots,<sup>1</sup> which reflects the band gap of the nanomaterials. Again, one can see that this value is very consistent with the result from the aforementioned voltammetric and fluorescence measurements. Additionally, it is interesting that no absorption peak is observed with the Au<sub>11</sub>Cl<sub>3</sub>(PPh<sub>3</sub>)<sub>7</sub> particles (Figure 4), as discussed above.

**Conclusions.** In summary, undecagold clusters were synthesized and stabilized by alkanethiolate monolayers. It was found that the electronic energy of these subnanometer-sized particles is very sensitive to surface protecting ligands, which is reflected in optical absorption and fluorescence measurements. From voltammetric studies, the band gap energy of these particles was estimated to be between 1.4 and 1.8 eV depending on the specific surface ligands; this energy range was found to be consistent with that evaluated spectroscopically.

**Acknowledgment.** We are grateful to Professor J. Z. Zhang at the University of California–Santa Cruz for valuable discussions. This work was supported, in part, by the National Science Foundation (CAREER Award No. CHE-0092760), the ACS Petroleum Research Fund, and the SIU Materials Technology Center. S.C. is a Cottrell Scholar of the Research Corporation.

## References

- (1) (a) Alivisatos, A. P. *J. Phys. Chem.* **1996**, *100*, 13226. (b) Zhang, J. *Z. Acc. Chem. Res.* **1997**, *30*, 423.
- (2) Alivisatos, A. P.; Barbara, P. F.; Castleman, A. W.; Chang, J.; Dixon, D. A.; Klein, M. L.; McLendon, G. L.; Miller, J. S.; Ratner, M. A.; Rosky, P. J.; Stupp, S. I.; Thompson, M. E. *Adv. Mater.* **1998**, *10*, 1297.
- (3) Murray, C. B.; Norris, D. J.; Bawendi, M. G. *J. Am. Chem. Soc.* **1993**, *115*, 8706.
- (4) Schaaff, T. G.; Shafiqullin, M. N.; Khoury, J. T.; Vezmar, I.; Whetten, R. L.; Cullen, W. G.; First, P. N. *J. Phys. Chem. B* **1997**, *101*, 7885.
- (5) Chen, S.; Ingram, R. S.; Hostetler, M. J.; Pietron, J. J.; Murray, R. W.; Schaaff, T. G.; Khoury, J. T.; Alvarez, M. M.; Whetten, R. L. *Science (Washington, D.C.)* **1998**, *280*, 2098.

- (6) Brust, M.; Walker, M.; Bethell, D.; Schiffrin, D. J.; Whyman, R. *J. Chem. Soc., Chem. Commun.* **1994**, 801.
- (7) Hostetler, M. J.; Wingate, J. E.; Zhong, C.-Z.; Harris, J. E.; Vachet, R. W.; Clark, M. R.; Londono, J. D.; Green, S. J.; Stokes, J. J.; Wignall, G. D.; Glish, G. L.; Porter, M. D.; Evans, N. D.; Murray, R. W. *Langmuir* **1998**, *14*, 17.
- (8) (a) Bigioni, T. P.; Whetten, R. L.; Dag, Ö. *J. Phys. Chem. B* **2000**, *104*, 6983. (b) Link, S.; Beeby, A.; FitzGerald, S.; El-Sayed, M. A.; Schaaff, T. G.; Whetten, R. L. *J. Phys. Chem. B* **2002**, *106*, 3410.
- (9) Huang, T.; Murray, R. W. *J. Phys. Chem. B* **2001**, *105*, 12498.
- (10) Bartlett, P. A.; Bauer, B.; Singer, S. J. *J. Am. Chem. Soc.* **1978**, *100*, 5085. The synthesis of other ultrasmall gold particles (e.g., Au<sub>13</sub>, Au<sub>55</sub>, etc.) was also reported previously (Smith, B. A.; Zhang, J. Z.; Giebel, U.; Schmid, G. *Chem. Phys. Lett.* **1997**, *270*, 139).
- (11) Woehrle, G. H.; Warner, M. H.; Hutchison, J. E. *J. Phys. Chem. B* **2002**, *106*, 9979.
- (12) *Inorganic Syntheses*; Ginsberg, A. P., Ed.; Wiley & Sons: New York, 1990; Vol. 27.
- (13) Chen, S.; Truax, L. A.; Sommers, J. M. *Chem. Mater.* **2000**, *12*, 3864.
- (14) Haram, S. K.; Quinn, B. M.; Bard, A. J. *J. Am. Chem. Soc.* **2001**, *123*, 8860.
- (15) (a) Kreibig, U.; Fauth, K.; Granqvist, C.-G.; Schmid, G. *Z. Phys. Chem. (Munich)* **1990**, *169*, 11. (b) Fauth, K.; Kreibig, U.; Schmid, G. *Z. Phys. D: At., Mol. Clusters* **1991**, *20*, 297. (c) Chi, L. F.; Hartig, M.; Schwaack, T.; Seidel, C.; Schmid, G. *Appl. Phys. A* **1998**, *66*, S187
- (16) *CRC Handbook of Chemistry and Physics*, 76th ed.; Lide, D. R., Ed.; CRC Press: Boca Raton, FL, 1995.
- (17) *Inorganic Electronic Structure and Spectroscopy*; Lever, A. B. P., Solomon, E. I., Eds.; Wiley & Sons: New York, 1999; Vol. 1, p 1.
- (18) Control experiments were also carried out with the Au(I) precursor (Au(PPh<sub>3</sub>)Cl) and the PPh<sub>3</sub> monomer, and no photoluminescence was observed within the wavelength range shown in Figure 2.
- (19) In Murray's study,<sup>9</sup> the excitation wavelength was set at 451 nm whereas in the present case, 680 nm. From Figure 4, one can see that the optical density of this Au<sub>11</sub>C12 particle solution at 451 nm is about 4 times that at 680 nm. With this difference, the efficiency of the photoluminescence of Au<sub>11</sub>C12 particles is estimated to be about 4 orders of magnitude smaller than that of tiopionin-protected gold particles.

NL025809J